

Studies of ferroelectric and magnetic phase transitions in multiferroic $\text{PbFe}_{0.5}\text{Ta}_{0.5}\text{O}_3\text{--PbTiO}_3$ solid solution ceramics

I. P. Raevski · V. V. Titov · M. A. Malitskaya · E. V. Eremin · S. P. Kubrin ·
A. V. Blazhevich · H. Chen · C.-C. Chou · S. I. Raevskaya · I. N. Zakharchenko ·
D. A. Sarychev · S. I. Shevtsova

Received: 15 March 2014 / Accepted: 31 May 2014 / Published online: 19 June 2014
© Springer Science+Business Media New York 2014

Abstract Dielectric, X-ray, Mossbauer and magnetization studies of $(1-x)\text{PbFe}_{0.5}\text{Ta}_{0.5}\text{O}_3\text{--}(x)\text{PbTiO}_3$ ceramics with $0 \leq x \leq 0.3$ have been carried out to determine the compositional evolution of ferroelectric and magnetic phase transition temperatures. Addition of PbTiO_3 to $\text{PbFe}_{0.5}\text{Ta}_{0.5}\text{O}_3$ increases the temperature T_m of the dielectric permittivity maximum, decreases both the diffusion of this maximum and its frequency dependence. However, the Curie–Weiss temperature exceeds T_m for all the compositions studied, indicating that the phase transition still remains diffused. Dilution of the (Fe, Ta)-sublattice by Ti lowers the Neel temperature T_N but above a certain compositional threshold ($x \approx 0.1$) fast lowering of T_N stops and a new magnetic state stable in a rather wide compositional range appears. Large difference between the

zero-field-cooled (ZFC) and FC magnetization–temperature curves as well as between the temperatures of magnetic phase transition determined from Mossbauer and magnetization studies for compositions with $x > 0.1$ implies that this state is a spin-glass phase.

Introduction

Single-phase multiferroics are the substances possessing simultaneously ferroelectric and magnetic properties [1–3]. Recent burst of interest to multiferroics has the aim to find materials, which can be used to convert the magnetic signals to electric responses and vice versa [1–4]. Among the best candidates for such applications are solid solutions of a ternary perovskite $\text{PbFe}_{0.5}\text{Ta}_{0.5}\text{O}_3$ (PFT). Recently

I. P. Raevski (✉) · V. V. Titov · M. A. Malitskaya ·
S. P. Kubrin · A. V. Blazhevich · S. I. Raevskaya ·
I. N. Zakharchenko · D. A. Sarychev · S. I. Shevtsova
Faculty of Physics and Research Institute of Physics, Southern
Federal University, Stachki Ave. 194, 344090 Rostov-on-Don,
Russia
e-mail: igorraevsky@gmail.com

V. V. Titov
e-mail: vvtitov@sfedu.ru

M. A. Malitskaya
e-mail: mamalitskaya@sfedu.ru

S. P. Kubrin
e-mail: stasskp@gmail.com

A. V. Blazhevich
e-mail: avblazhevich@sfedu.ru

S. I. Raevskaya
e-mail: siraevskaya@sfedu.ru

I. N. Zakharchenko
e-mail: inzakharchenko@sfedu.ru

D. A. Sarychev
e-mail: dasarychev@sfedu.ru

S. I. Shevtsova
e-mail: sishevtsova@sfedu.ru

E. V. Eremin
Kirensky Institute of Physics, Siberian Branch of the Russian
Academy of Sciences, Akademgorodok, 38,
660036 Krasnoyarsk, Russia
e-mail: eev@iph.krasn.ru

H. Chen
Faculty of Science and Technology, University of Macau,
Av. Padre Tomas Pereira, Macao, China
e-mail: HaydnChen@umac.mo

C.-C. Chou
National Taiwan University of Science and Technology,
Keelung Road, 43, 106 Taipei, Taiwan
e-mail: ccchou@mail.ntust.edu.tw

$(1-x)\text{PbFe}_{0.5}\text{Ta}_{0.5}\text{O}_{3-x}\text{Pb}(\text{Zr}, \text{Ti})\text{O}_3$ (PFT- x PZT) solid solution ceramics with $x = 0.6\text{--}0.7$ were reported to possess at room-temperature magnetic hysteresis loops, saturated at ≈ 0.1 emu/g and relatively low dielectric losses, which is a great advantage for magnetoelectric devices [4]. However, the data on the magnetic phase transitions in PFT and especially in PFT solid solutions are rather fragmentary and contradictory.

On cooling, PFT undergoes a sequence of phase transitions: from the cubic paraelectric to tetragonal ferroelectric phase at $T_{\text{CT}} \approx 270$ K, then to the monoclinic ferroelectric phase, at $T_{\text{TM}} \approx 200\text{--}220$ K, and, finally, to the G-type antiferromagnetic (AFM) phase at $130\text{--}180$ K [5–11]. Besides the AFM phase transition PFT exhibits also the lower-temperature magnetic anomaly at $T_{\text{g}} \approx 9\text{--}16$ K corresponding to the transition into a spin glass state [3, 8, 9]. The temperature of the AFM phase transition (the Neel temperature, T_{N}) determined in different works varies for PFT from 130 to 180 K [7, 10, 11]. The temperature of magnetic phase transition in Fe-containing oxides is believed to depend on the number of possible Fe–O–Fe linkages in a crystal lattice [12]. In ternary $\text{PbFe}_{0.5}\text{B}_{0.5}^{5+}\text{O}_3$ perovskites this number can be governed, e.g., by changing the degree of Fe^{3+} and B^{5+} cations ordering, because such ordering reduces the possible number of Fe–O–Fe linkages. However, in contrast to $\text{PbB}_{0.5}^{3+}\text{B}_{0.5}^{5+}\text{O}_3$ perovskites with $\text{B}^{3+} = \text{Sc}, \text{Yb}$, $\text{B}^{5+} = \text{Nb}, \text{Ta}$ [13, 14], no superstructure reflections on X-ray diffraction (XRD) patterns due to Fe^{3+} and Ta^{5+} ordering have been reported for PFT [5–8]. At the same time, the experimental value of T_{N} for PFT is located approximately halfway between calculated values for the fully ordered ($T_{\text{N}} = 0$ K) and completely disordered ($T_{\text{N}} \approx 300$ K) states [7] which is usually interpreted as an evidence of a partial ordering of Fe^{3+} and Ta^{5+} cations [7]. The possible reason for the absence of superstructural reflections on XRD patterns is believed to be a local mesoscopic character of ordering in PFT. Temperatures of magnetic phase transitions in PFT and in its analog, $\text{PbFe}_{0.5}\text{Nb}_{0.5}\text{O}_3$ (PFN), exhibiting the same sequence of structural and magnetic phase transitions, are more than 100 K higher compared to similar lead-free $\text{AFe}_{0.5}\text{B}_{0.5}\text{O}_3$ (A: Ca, Sr, Ba, B: Nb, Ta) perovskites [15]. This dramatic difference is believed to be due to the possibility of magnetic superexchange via an empty 6p state of Pb^{2+} ions [15] or to the clustering of Fe ions [16]. According to first-principle calculations [16] clustering of Fe ions appears to be more probable in $\text{PbFe}_{0.5}\text{B}_{0.5}\text{O}_3$ (B: Nb, Ta) compounds than in their lead-free counterparts. So the possible reason of large scattering of T_{N} values obtained for PFT in different works seems to be local compositional ordering and/or clustering of Fe ions. Studies of ^{93}Nb and ^{17}O NMR [17] and ^{57}Fe

Mossbauer spectra [16] as well as magnetization studies [3] and first-principal calculations [16] have led to the conclusion that PFN is chemically inhomogeneous system and long-range AFM order develops in Fe-rich–Nb-poor regions while, a magnetic relaxor spin-glass-like state below $T \approx 10\text{--}20$ K can arise from the Fe-poor–Nb-rich regions. Similar scenario seems to be valid for PFT.

In several works magnetic hysteresis loops were observed in PFT [9, 18], PFT- x PT [18], and PFT- x PZT [4] ceramics at ambient temperature. The existence of these loops is usually explained by the presence of super-AFM and/or superparamagnetic clusters far above the ambient temperature [4, 9]. However, in [18] it was supposed that ferromagnetic (or ferrimagnetic) properties of PFT and PFT-0.2PT ceramics are due to the presence in the samples of the admixture of pyrochlore $\text{Pb}_3\text{FeTaO}_7$ phase. This conclusion was based on the fact that in $\text{Pb}_3\text{FeTaO}_7$ ceramics magnetic hysteresis loops at room temperature were observed also and the remnant magnetization values appeared to be much larger than those for PFT and PFT-0.2PT ceramics [18].

The scope of the present paper is the study of the compositional evolution of ferroelectric and magnetic phase transition temperatures in $(1-x)\text{PFT}-(x)\text{PbTiO}_3$ solid solution ceramics within the $0 \leq x \leq 0.3$ range.

Materials and methods

Ceramic samples of $(1-x)\text{PFT}-(x)\text{PbTiO}_3$ (PFT- x PT) have been obtained by one-stage sintering process via a solid-state reaction route using high-purity Fe_2O_3 , PbO , TiO_2 , and Ta_2O_5 as starting oxides. This method is known to be even more effective for fabricating the single-phase perovskite PFT ceramics as compared to a multi-stage process including the preliminary synthesis of FeTaO_4 precursor, intermediate synthesis of PFT at $800\text{--}900$ °C, and final sintering at higher temperature [19, 20]. The starting oxides were batched in stoichiometric proportions, and 1 wt% Li_2CO_3 was added to the batch. This addition is known to promote formation of the perovskite modification of PFN and its solid solutions and to reduce dramatically their conductivity [21, 22]. Also 5 mol% excess of PbO was added to the batch in order to compensate PbO losses during sintering. After mixing thoroughly in an agate mortar under ethyl alcohol and subsequent drying, the green ceramic samples were pressed at 100 MPa in the form of disks of 10 mm in diameter and of 3–4 mm in height using polyvinyl alcohol as a binder. The sintering was performed at $1050\text{--}1150$ °C for 2 h in a closed alumina crucible. PMN powder was used to create PbO buffer atmosphere. The density of the obtained ceramics was

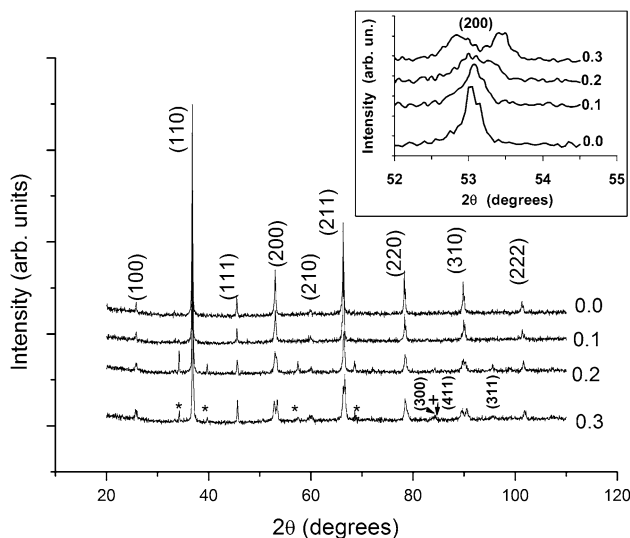


Fig. 1 X-ray diffraction patterns for PFT-*x*PT ceramics at room temperature. Numbers at the curves correspond to *x* values. Asterisks mark the reflections corresponding to the pyrochlore phase. The inset highlights evolution of the (200) reflection with composition

about 92–96 % of the theoretical one. The average grain size determined by a linear intercept method was around 5–7 μm for PFT ceramics and 10–12 μm for PFT-*x*PT compositions studied. The electrodes for measurements were deposited on the grinded disks of 8–9 mm in diameter and of 0.8–0.9 mm in height by firing on silver past. Dielectric studies were carried out in the 10²–10⁶ Hz range in the course of both heating and cooling at a rate of 2–3 K/min with the aid of the computer-controlled E7-20 and Novocontrol Alpha-A impedance meters. Mossbauer spectra were recorded with the aid of the MS-1104E rapid spectrometer and analyzed using the original computer program UNIVEM. Magnetic measurements were performed using the PPMS-9 physical property measurement system (Quantum Design) in the temperature range 2–300 K and under magnetic field up to 90 kOe.

The XRD studies were performed on a DRON 3.0 diffractometer (Co Kα radiation, θ–2θ scan mode).

Results

Room-temperature XRD studies have shown that Li-doped PFT ceramics is single-phase and has a cubic perovskite structure (Fig. 1). PFT-*x*PT compositions with *x* > 0.1 contained a small amount of the pyrochlore phase, presumably Pb₃FeTaO₇ [18]. The volume percent of pyrochlore phase β, was estimated from the ratio of relative intensities of the (222) pyrochlore peak (I₂₂₂)_{PYRO} and the (110) perovskite peak (I₁₁₀)_{PER} [23]:

$$\beta = \frac{(I_{222})_{PYRO}}{(I_{222})_{PYRO} + (I_{110})_{PER}} \cdot 100 \%$$

Thus obtained β values were ≈9 and ≈4 % for *x* = 0.2 and 0.3 compositions, respectively. Similar pyrochlore content was reported for PFT–0.2PT ceramic composition obtained by a two-stage sintering process via a solid-state reaction route [18].

As was already mentioned, PFT possesses a tetragonal symmetry in the 220–270 K temperature range [5, 6]. Addition of tetragonal PT to PFT is expected to increase the tetragonal–cubic phase transition temperature T_{CT}. Linear extrapolation of the T_{CT} of PFT (≈270 K) to that of PT (≈760 K) predicts the appearance of tetragonal phase at 300 K for compositions with *x* > 0.07. However, tetragonal splitting of the (200) reflection becomes visible only for *x* = 0.3 composition (Fig. 1). Nevertheless the (200) diffraction peak gradually widens as *x* grows from 0 to 0.2 (inset in Fig. 1). This widening seems to be a fingerprint of the coexistence of cubic and tetragonal phases.

Similar to other AFe_{0.5}B_{0.5}O₃ (A: Ba, Sr, Ca, Pb, B: Nb, Ta) perovskites, electric conductivity of undoped PFT ceramics depends dramatically on the sintering temperature and thus fabrication of PFT-based ceramics with low conductivity is a rather difficult task. Li-doping was approved to be an effective method of increasing the resistivity of PFN and its solid solutions [21, 22]. We found out that similar to PFN-based compositions, Li-doping decreases the conductivity of PFT-*x*PT ceramics dramatically. Figure 2 shows the temperature dependences of dielectric permittivity ε and loss tangent tanδ for highly resistive Li-doped PFT-*x*PT ceramics measured at 1 kHz. One can see that the samples obtained possess very high permittivity maxima (1.5–2 times higher than the ones reported in the literature [9, 18, 24–26]) and rather low tanδ values. It is worth noting that comparable height of the ε(*T*) maximum for undoped PFT ceramics has been obtained in [20] by a long-time annealing at high temperatures. Temperature T_m of the ε(*T*) maximum (at 1 kHz) of Li-doped PFT ceramics (Fig. 2, curve 1) is similar to that reported in literature for PFT single crystals and undoped PFT ceramics [7, 9, 11, 18, 20, 24–26]. Similar to single crystals and undoped PFT ceramics [7, 9, 11, 18, 24–26] Li-doped PFT ceramics exhibit relaxor-like properties—a diffused and frequency-dependent ε(*T*) maximum. The T_m frequency shift, Δ*T* = T_m(10⁶ Hz) – T_m(10² Hz) for Li-doped PFT ceramics (Fig. 3) is comparable with Δ*T* values reported for undoped PFT ceramics [9, 20]. For PFT-*x*PT compositions T_m increases (Figs. 2, 3), the ε(*T*) maximum becomes sharper (Fig. 2), and its frequency shift Δ*T* diminishes as *x* grows and practically vanishes for *x* = 0.3 (Fig. 3). These results qualitatively agree with the data reported earlier for PFT–0.2PT composition [18]. To

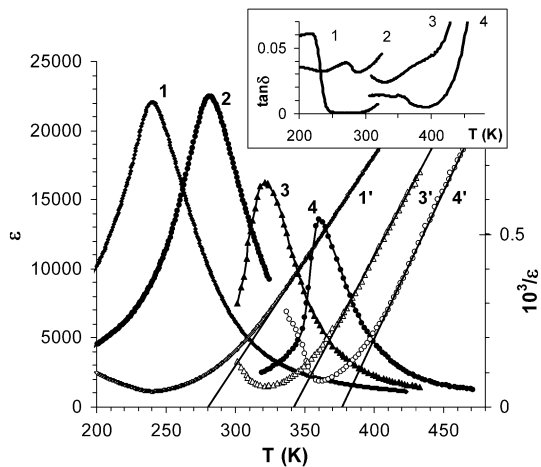


Fig. 2 Temperature dependences of permittivity measured at 1 kHz (1–4) and reciprocal permittivity ($1'$, $3'$, $4'$) for Li-doped PFT- x PT ceramic compositions with $x = 0$ (1, $1'$), 0.1 (2), 0.2 (3, $3'$), and 0.3 (4, $4'$). The inset shows temperature dependences of $\tan\delta$ at 1 kHz for the same compositions

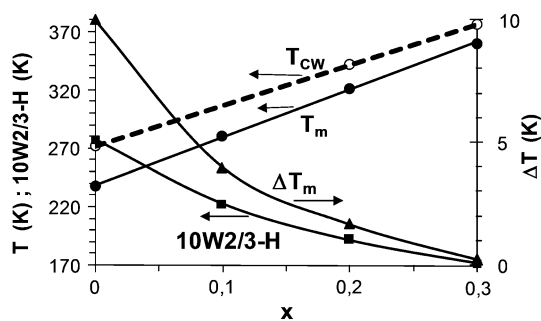


Fig. 3 Dependence of permittivity maximum temperature T_m , extrapolated Curie-Weiss temperature T_{CW} , T_m frequency shift ΔT and the parameter $W_{2/3}M - H$ characterizing diffusion of the $\varepsilon(T)$ maximum (see text for details), on the composition for Li-doped PFT- x PT ceramics. Note that $W_{2/3}M - H$ values are multiplied by factor 10 in order to match the scale used

estimate quantitatively the diffuseness of the $\varepsilon(T)$ maximum we used the parameter $W_{2/3}M - H$, defined as the difference between T_m and the temperature where ε reaches 2/3 of the maximum value from the high-temperature side of the peak [27]. The value of $W_{2/3}M - H$ was shown [27] to be very close to the diffusion parameter δ , calculated using a quadratic formula [28]. Thus obtained $W_{2/3}M - H$ values for PFT-PT ceramics decrease monotonically with x (Fig. 3). However, even for PFT-0.3PT composition the $W_{2/3}M - H$ value (17 K) is somewhat larger than the value 12 K reported for the composition with the same PT content in the PFN- x PT system [22].

For all the PFT- x PT compositions studied, the linear Curie-Weiss (CW) law is fulfilled at temperatures exceeding T_m by 40–50 K (Fig. 2). However, the

extrapolated CW temperature T_{CW} appears to be substantially higher than T_m (Fig. 3) which is typical of relaxors and ferroelectrics with a diffused phase transition. Addition of PbTiO_3 leads to decrease of the difference between T_{CW} and T_m but this difference persists even for PFT-0.3PT despite the fact that T_m frequency shift ΔT is practically 0 for this composition (Fig. 3). Thus the Li-doped PFT-0.3PT ceramic composition exhibits, from one side, the features typical of usual ferroelectrics [slightly diffused $\varepsilon(T)$ maximum, absence of the frequency shift of T_m] and, from the other side, properties characteristic of relaxors and ferroelectrics with diffuse phase transition (the linear CW law is valid only at temperatures much higher than T_m with $T_{CW} > T_m$). Similar combination of contradictory properties was reported for $0.5\text{PbMg}_{1/3}\text{Nb}_{2/3}\text{O}_3$ - 0.5PbTiO_3 single crystals [29] where the structural phase transition takes place at T_m and neither conventional relaxor dispersion, nor the frequency shift of T_m are observed. Nevertheless, the universal relaxor dispersion still persists in these crystals and T_m corresponds not to the ferroelectric-paraelectric but rather to the ferroelectric-relaxor phase transition [29].

At room temperature Mossbauer ^{57}Fe spectra of all the compositions studied appeared to be doublets with quadrupole splitting of ≈ 0.4 mm/s and isomer shift of ≈ 0.4 mm/s (relative to metallic iron), corresponding to the Fe^{3+} ions occupying the octahedral sites of perovskite lattice (Fig. 4). When cooling below the Neel temperature, T_N , the Mossbauer spectrum transforms from doublet to sextet [11, 15, 30]. This transformation is accompanied by a dramatic decrease of the magnitude η of Mossbauer spectra intensity within the 0–1.2 mm/s velocity range normalized to its value at 300 K (Fig. 5). This abrupt drop in the temperature dependence of η allows one to obtain T_N from the Mossbauer experiment. It is worth noting that finite η values observed at $T < T_N$ (Fig. 5) are due not only to the presence of a part of iron ions in the magnetically disordered state, but rather also to the contribution of the sextet component of the spectrum falling within the 0–1.2 mm/s velocity range. This method was successfully used previously to determine values of T_N in several multiferroics and their solid solutions and the results obtained were very similar to the data obtained by traditional methods such as the magnetization or magnetic susceptibility measurements (see [15, 30] and references therein). Li-doping is known to stimulate the compositional ordering in ternary $\text{PbB}_{0.5}^{3+}\text{B}_{0.5}^{5+}\text{O}_3$ perovskites [11, 13]. Such ordering may decrease dramatically the T_N values due to reducing the number of the neighboring magnetic Fe^{3+} ions around the given Fe^{3+} ion. Indeed, Li-doped PFT ceramics exhibit a large scatter of T_N values, depending on the sintering temperature [11]. In the present study, we used two samples of Li-doped PFT ceramics—one was

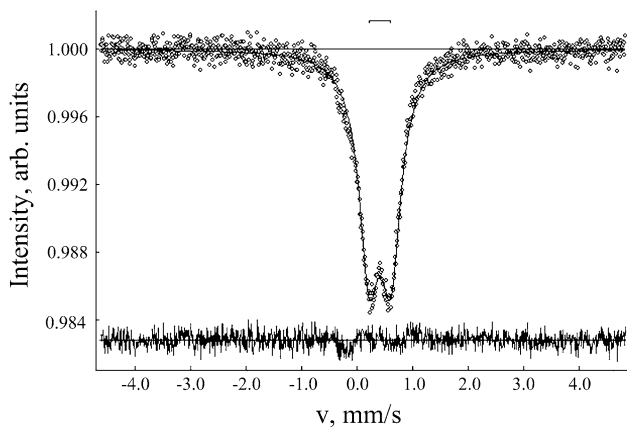


Fig. 4 Mossbauer spectrum of the PFT–0.1PT composition at 300 K. Points mark the experimental data, solid line is the result of fitting the spectrum by one doublet. The line at the bottom shows the difference between experimental and simulated data

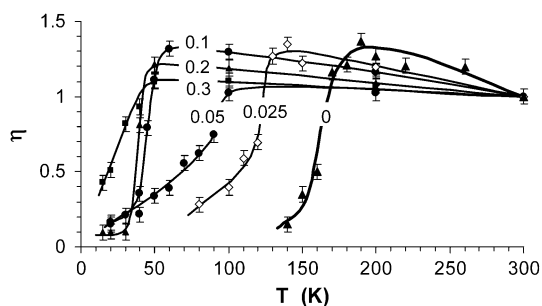
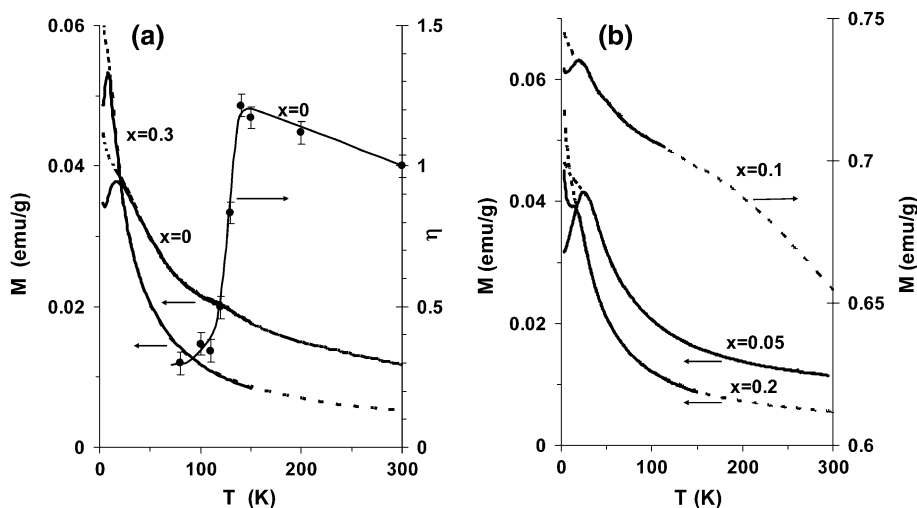


Fig. 5 Temperature dependences of η -Mossbauer spectrum intensity within the 0–1.2 mm/s velocity range, related to its value at 300 K, for several Li-doped PFT– x PT compositions. Numbers at the curves correspond to x values

sintered at 1150 °C and had $T_N \approx 160$ –170 K (Fig. 5, curve 0) which corresponds well to the majority of the data published for PFT [7, 11, 24]. The other sample was

Fig. 6 Temperature dependences of magnetization M measured under a magnetic field of 1 kOe in the ZFC (solid lines) and FC (broken lines) modes and η -Mossbauer spectrum intensity within the 0–1.2 mm/s velocity range, related to its value at 300 K, for several compositions of Li-doped PFT– x PT ceramics

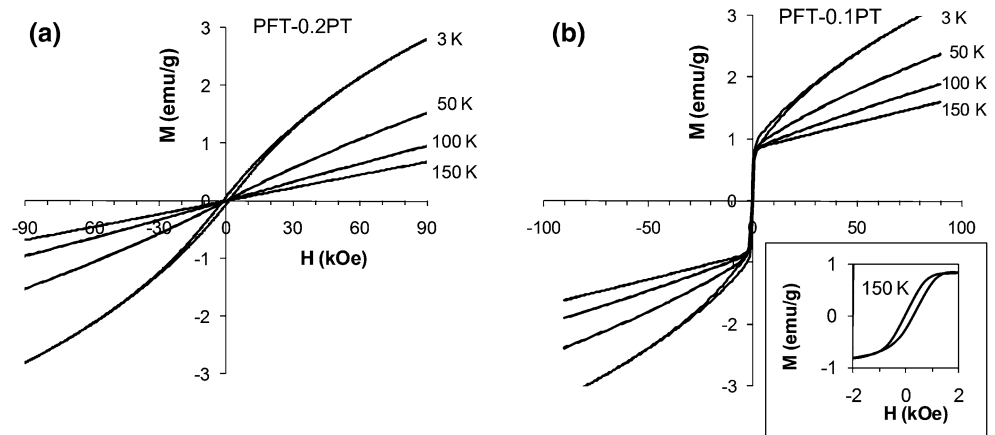


sintered at 1080 °C and, according to results of Mossbauer and magnetization studies, had a substantially lower $T_N \approx 130$ K (Fig. 6a). As was already mentioned above, this difference in T_N values can originate from the changes in the degree of Fe clustering in the lattice [16].

One can see from Fig. 5 that the temperature of the abrupt drop of the $\eta(T)$ curves lowers as x grows. This dependence will be discussed below in more detail.

There are some data on the temperature dependences of magnetization (M) for PFT single crystals and ceramics in the literature [7–9, 24]. In the present work, we studied the $M(T)$ dependences of Li-doped PFT– x PT ceramics (Fig. 6). For $x = 0$ composition the $M(T)$ dependence is very similar to the one observed for PFT and PFN single crystals: during heating under a magnetic field of 1 kOe after zero-field-cooling (ZFC) it has a maximum at 16 K (Fig. 6a). Besides this maximum there is also a bump on the $M(T)$ curve at about 130 K corresponding to T_N . One can see in Fig. 6a, that the temperature of the bump in the $M(T)$ curve for Li-doped PFT ceramics nicely coincides with the $\eta(T)$ anomaly for the same sample. For all the compositions studied the $M(T)$ dependence measured in the FC mode is very close to the one measured in the ZFC mode except a low-temperature region where the FC curve does not show a maximum. Such a difference between the $M(T)$ curves measured in the ZFC and FC modes is typical of a spin-glass state [3, 8, 24]. For compositions with $x \geq 0.05$ only the low-temperature maximum is observed in the $M(T)$ curves measured in the ZFC mode (Fig. 6). This is typical of solid solutions of multiferroics, where a small bump, corresponding to T_N , usually diffuses and finally disappears on increasing the concentration of the nonmagnetic component [31]. For example, in the PFN– x PT ceramics a bump corresponding to T_N is observed only for compositions with $x \leq 0.04$ [31]. However, the anomalies on the $\eta(T)$ curves are well seen for all the PFT– x PT compositions studied (Fig. 5).

Fig. 7 Magnetic hysteresis loops at different temperatures for Li-doped PFT–0.2PT (a) and PFT–0.1PT (b) ceramics. The inset in b shows the low-field portion of the hysteresis loop for PFT–0.1PT composition at 150 K



All the Li-doped PFT– x PT ceramic compositions studied except $x = 0.1$ exhibited slim magnetic hysteresis loops at very low temperatures of about few K (Fig. 7a). However, at 50 K, the $M(H)$ dependences showed only a slight nonlinearity, while at higher temperatures, namely at 100 and 150 K they were practically linear. Thus the evolution of magnetic hysteresis loops with temperature for Li-doped PFT– x PT ceramics is very similar to the data obtained for PFN single crystal [32]. However, one of the samples studied (PFT–0.1PT) exhibited unusually high magnetization values which were more than an order of magnitude larger as compared to the other compositions studied. Both the ZFC and FC magnetization–temperature curves for this sample were much more diffused than the ones for the other samples studied. For the $x = 0.1$ composition the ratio of the $M(T)$ maximal value to the M value at 300 K in the ZFC curve is about 1.12, while for all the other compositions studied, the same ratio is substantially larger and varies from 3.23 to 10.33. Moreover, the PFT–0.1PT sample exhibited the well-defined magnetic hysteresis $M(H)$ loops up to at least 150 K (Fig. 7b), i.e., well above the temperature of magnetic ordering for this composition determined from the $\eta(T)$ anomaly (Fig. 5). As these loops change rather weakly from 50 to 150 K it seems that they would exist at room temperature as well. Note that no reflexes of pyrochlore phase are observed on the XRD pattern for the PFN–0.1PT composition studied (Fig. 1). Mossbauer spectrum of this sample also did not show any traces of ferro- or ferrimagnetic sextet components (Fig. 4). On the other hand PFT–0.2PT and PFT–0.3PT compositions which contain an admixture of the pyrochlore phase exhibit magnetic hysteresis loops only at very low temperatures and the form of these loops differs from those observed for PFN–0.1PT sample. Thus our data do not support the assumption on the relation of the room-temperature ferro (or ferri)-magnetic properties of PFT– x PT with the presence of the admixture of the pyrochlore phase in the samples. It is worth noting that high M values

as well as $M(T)$ and $M(H)$ dependences, very similar to those observed for PFT–0.1PT composition, have been reported recently for PFT ceramic sample studied in [9]. We suppose that such unusual behavior is due to the presence in the Li-doped PFT–0.1PT sample a small amount of ferrimagnetic impurity, presumably $\text{PbFe}_{12}\text{O}_{19}$ and/or LiFe_5O_8 . Although the content of this impurity seems to be well below the detection limit of the XRD and Mossbauer spectroscopy, ferrimagnetic impurity has a great impact on the magnetic properties of the AFM or paramagnetic matrix. This assumption is supported by the fact that very similar diffused $M(T)$ curves were observed for the magneto-electric composite based on ferrimagnetic $\text{Ni}_{0.3}\text{Zn}_{0.62}\text{Cu}_{0.08}\text{Fe}_2\text{O}_4$ ferrite as a magnetostrictive phase and $\text{Pb}(\text{Fe}_{0.5}\text{Nb}_{0.5})\text{O}_3$ as a piezoelectric phase [33].

In the PFT– x PT compositions studied the temperature T_g of the $M(T)$ maximum at first increases as x grows but at larger x values decreases (Fig. 6). It is worth noting that a similar increase of T_g with x growing was observed previously for the PFN– x PT ceramics in the $x < 0.1$ compositional range [31]. This increase was attributed to a slight decrease of the lattice parameter with x and a subsequent increase of the magnetic coupling. However, the similar character of the $T_g(x)$ dependence was observed later for the PFN– $x\text{BaFe}_{0.5}\text{Nb}_{0.5}\text{O}_3$ solid solutions where the lattice parameter increases with x [32]. We suppose that the observed increase of T_g in both PFN– x PT and PFT– x PT systems is a result of the increase of the average size of the confined percolation clusters, with x , because of the decrease of the strength of the infinite cluster [32].

The results of Mossbauer and magnetization studies for both PFN– x PT and PFT– x PT solid solution systems are summarized in Fig. 8. According to Mossbauer data, at low x values T_N rapidly decreases as x grows. Lowering of T_N with x in both systems is quite expectable due to dilution of the magnetic subsystem. However, above a certain compositional threshold ($x \approx 0.1$) fast lowering of T_N with the increase of the Ti concentration stops and a new magnetic

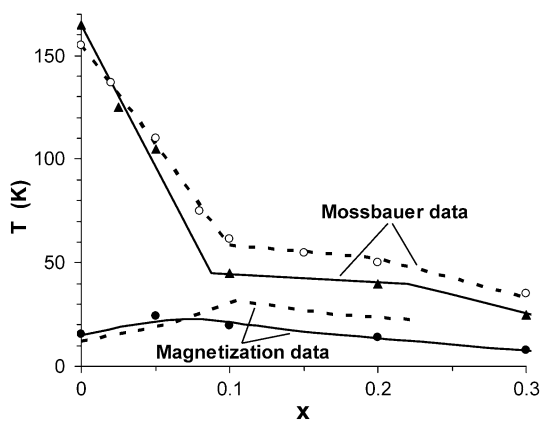


Fig. 8 Compositional dependences of the temperatures of the $\eta(T)$ anomaly and the maximum of the magnetization–temperature dependence in the ZFC mode for PFT– x PT (solid lines) and PFN– x PT (broken lines) ceramics. Magnetization data for PFN– x PT are plotted using the data of [31] for ceramics and [32] for single crystals

state with comparatively high (~ 50 K) transition temperature becomes stable in a rather wide compositional range (Fig. 8). According to magnetization data, in this compositional range ($x > 0.1$) the magnetic state is a spin-glass-like one. In both PFN– x PT and PFT– x PT systems T_g values are lower by about 20 K than the temperatures of magnetic phase transition determined from the Mossbauer studies. This difference seems to be caused by the fact that the upper limit of the spin relaxation rates in these samples is above the characteristic Mossbauer time [34]. Similar behavior was reported e.g., for $\text{PbFe}_{12-x}\text{Cr}_x\text{O}_{19}$ hexaferrites [35].

Conclusions

In conclusion, highly resistive Li-doped $(1-x)\text{PbFe}_{0.5}\text{Ta}_{0.5}\text{O}_3-(x)\text{PbTiO}_3$ ceramics ($0 \leq x \leq 0.3$) with high dielectric permittivity maxima and low losses were obtained by one-step sintering. Addition of PbTiO_3 to $\text{PbFe}_{0.5}\text{Ta}_{0.5}\text{O}_3$ increases the temperature T_m of the permittivity maximum and decreases substantially the diffusion of this maximum. Nevertheless, within the composition range studied, ferroelectric phase transition remains diffuse as is evidenced by the fact that the extrapolated CW temperature exceeds T_m . No relation was revealed between the room-temperature ferro (or ferri)-magnetic properties of PFT– x PT and the presence of the admixture of the pyrochlore phase in the samples. Dilution of Fe sublattice by Ti lowers the Neel temperature T_N . However, above a certain compositional threshold ($x \approx 0.1$) fast lowering of T_N stops and a new magnetic state stable in a rather wide compositional range appears. Large difference between the ZFC and FC

magnetization curves as well as between the temperature of magnetic phase transition determined from Mossbauer studies and the temperature T_g of the ZFC magnetization curve maximum for compositions with $x > 0.1$ implies that this state is a spin-glass phase.

We suppose that both the maximum of the $T_g(x)$ dependence and a sharp change of the slope of $T_N(x)$ dependence at $x \approx 0.1$ are the fingerprints of a percolation phase transition in the $(1-x)\text{PbFe}_{0.5}\text{Ta}_{0.5}\text{O}_3-(x)\text{PbTiO}_3$ solid solution system. Similar transition was revealed recently in the $(1-x)\text{PbFe}_{0.5}\text{Nb}_{0.5}\text{O}_3-(x)\text{PbTiO}_3$ solid solution system [30, 32]. Since such a phase transition is a critical phenomenon, one may expect an enhancement of all physical responses in the crystal matrix, and, in particular, the enhancement of the magnetoelectric response near the compositional threshold ($x \approx 0.1$).

Acknowledgements This study is partially supported by the Russian Foundation for Basic Research (RFBR) Project 12-08-00887_a and Research Committee of the University of Macau under Research and Development Grant for Chair Professor.

References

1. Khomskii DI (2006) Multiferroics: different ways to combine magnetism and ferroelectricity. *J Magn Magn Mater* 306:1–8
2. Fiebig M (2005) Revival of the magnetoelectric effect. *J Phys D* 38:R123–R152
3. Kleemann W, Shvartsman VV, Borisov P, Kania A (2010) Coexistence of antiferromagnetic and spin cluster glass order in the magnetoelectric relaxor multiferroic $\text{PbFe}_{0.5}\text{Nb}_{0.5}\text{O}_3$. *Phys Rev Lett* 105:257202-1–257202-4
4. Sanchez DA, Ortega N, Kumar A et al (2011) Symmetries and multiferroic properties of novel room-temperature magnetoelectrics: lead iron tantalate–lead zirconate titanate (PFT/PZT). *AIP Adv* 1:042169-1–042169-14
5. Lehmann AG, Sciau P (1999) Ferroelastic symmetry changes in the perovskite $\text{PbFe}_{0.5}\text{Ta}_{0.5}\text{O}_3$. *J Phys Condens Matter* 11:1235–1245
6. Lampis N, Sciau P, Lehmann AG (2000) Rietveld refinements of the paraelectric and ferroelectric structures of $\text{PbFe}_{0.5}\text{Ta}_{0.5}\text{O}_3$. *J Phys Condens Matter* 12:2367–2378
7. Nomura S, Takabayashi H, Nakagawa T (1968) Dielectric and magnetic properties of $\text{Pb}(\text{Fe}_{1/2}\text{Ta}_{1/2})\text{O}_3$. *Jpn J Appl Phys* 7:600–604
8. Falqui A, Lampis N, Geddo-Lehmann A, Pinna G (2005) Low-temperature magnetic behavior of perovskite compounds $\text{PbFe}_{1/2}\text{Ta}_{1/2}\text{O}_3$ and $\text{PbFe}_{1/2}\text{Nb}_{1/2}\text{O}_3$. *J Phys Chem B* 109:22967–22970
9. Martinez R, Palai R, Huhtinen H, Liu J, Scott JF, Katiyar RS (2010) Nanoscale ordering and multiferroic behavior in $\text{PbFe}_{1/2}\text{Ta}_{1/2}\text{O}_3$. *Phys Rev B* 82:134104-1–134104-10
10. Shvorneva LI, Venevtsev YuN (1965) Perovskites with ferromagnetic properties. *Sov Phys JETP* 22:722–725
11. Kubrin SP, Raevskaya SI, Kuropatkin SA, Raevski IP, Sarychev DA (2006) Dielectric and Mossbauer studies of B-cation order-disorder effect on the properties of $\text{Pb}(\text{Fe}_{1/2}\text{Ta}_{1/2})\text{O}_3$ relaxor ferroelectric. *Ferroelectrics* 340:155–159
12. Gilleo MA (1960) Superexchange interaction in ferromagnetic garnets and spinels which contain randomly incomplete linkages. *J Phys Chem Solids* 13:33–39

13. Bokov AA, Shonov VYu, Rayevsky IP, Gagarina ES, Kupriyanov MF (1993) Compositional ordering and phase transitions in $\text{PbYb}_{1/2}\text{Nb}_{1/2}\text{O}_3$. *J Phys Condens Matter* 5:5491–5504
14. Raevski IP, Prosandeev SA, Emelyanov SM et al (2004) Comparative study of cation ordering effects in single crystals of 1:1 and 1:2 complex perovskites solid solutions. *Ferroelectrics* 298:267–274
15. Raevski IP, Kubrin SP, Raevskaya SI et al (2009) Experimental evidence of the crucial role of nonmagnetic Pb cations in the enhancement of the Neel temperature in perovskite $\text{Pb}_{1-x}\text{Ba}_x\text{Fe}_{1/2}\text{Nb}_{1/2}\text{O}_3$. *Phys Rev B* 80:024108-1–024108-6
16. Raevski IP, Kubrin SP, Raevskaya SI et al (2012) Magnetic properties of $\text{PbFe}_{1/2}\text{Nb}_{1/2}\text{O}_3$: Mossbauer spectroscopy and first principles calculations. *Phys Rev B* 85:224412-1–224412-5
17. Laguta VV, Rosa J, Jastrabik L et al (2010) ^{93}Nb NMR and Fe^{3+} EPR study of local magnetic properties of disordered magnetoelectric $\text{PbFe}_{1/2}\text{Nb}_{1/2}\text{O}_3$. *Mater Res Bull* 45:1720–1727
18. Cho SY, Kim JS, Jang MS (2006) Dielectric, ferroelectric and ferromagnetic properties of $0.8\text{PbFe}_{0.5}\text{Ta}_{0.5}\text{O}_3$ – 0.2PbTiO_3 ceramics. *J Electroceram* 16:369–372
19. Shonov VYu, Raevski IP, Bokov AA (1996) Electrophysical properties of ferroelectric solid solutions $x\text{PbFe}_{1/2}\text{Ta}_{1/2}\text{O}_3$ – $y\text{PbFe}_{1/2}\text{Nb}_{1/2}\text{O}_3$ – $(1-x-y)\text{PbMg}_{1/3}\text{Nb}_{2/3}\text{O}_3$. *Zhurnal Tekhnicheskoi Fiziki* 66:98–102. *Engl Transl Tech Phys* 4:166–168 (in Russian)
20. Zhu WZ, Kholkin A, Mantas PQ, Baptista JL (2000) Preparation and characterization of $\text{Pb}(\text{Fe}_{1/2}\text{Ta}_{1/2})\text{O}_3$ relaxor ferroelectric. *J Eur Ceram Soc* 20:2029–2034
21. Raevski IP, Kirillov ST, Malitskaya MA et al (1988) Phase transitions and ferroelectric properties of lead ferroniobate. *Izv AN SSSR Neorg Mater* 24:286–289. *Engl Transl Inorg Mater* 24:217–220 (in Russian)
22. Sitalo EI, Raevski IP, Lutokhin AG et al (2011) Dielectric and piezoelectric properties of $\text{PbFe}_{1/2}\text{Nb}_{1/2}\text{O}_3$ – PbTiO_3 ceramics from the morphotropic phase boundary compositional range. *IEEE Trans Ultrason Ferroelectr Freq Control* 58:1914–1918
23. Swartz SL, Shrout TR (1982) Fabrication of perovskite lead magnesium niobate. *Mater Res Bull* 17:1245–1250
24. Choudhury RNP, Rodriguez C, Bhattacharya P, Katiyar RS, Rinaldi C (2007) Low-frequency dielectric dispersion and magnetic properties of La, Gd modified $\text{Pb}(\text{Fe}_{1/2}\text{Ta}_{1/2})\text{O}_3$ multiferroics. *J Magn Magn Mater* 313:253–260
25. Kulawik J, Szwagierczak D (2007) Dielectric properties of manganese and cobalt doped lead iron tantalate ceramics. *J Eur Ceram Soc* 27:2281–2286
26. Bormanis K, Burkhanov AI, Vaingolts AI, Kalvane A (2011) The effect of bias field on dielectric response in lead ferrotantalate ceramics. *Integr Ferroelectr* 123:144–147
27. Lei C, Bokov AA, Ye Z-G (2007) Ferroelectric to relaxor crossover and dielectric phase diagram in the BaTiO_3 – BaSnO_3 system. *J Appl Phys* 101:084105-1–084105-9
28. Bokov AA, Bing Y-H, Chen W et al (2003) Empirical scaling of the dielectric permittivity peak in relaxor ferroelectrics. *Phys Rev B* 68:052102-1–052102-4
29. Bokov A, Luo H, Ye Z-G (2005) Polar nanodomains and relaxor behaviour in $(1-x)\text{Pb}(\text{Mg}_{1/3}\text{Nb}_{2/3})\text{O}_3$ – $x\text{PbTiO}_3$ crystals with $x = 0.3$ – 0.5 . *Mater Sci Eng B* 120:206–209
30. Raevski IP, Kubrin SP, Raevskaya SI et al (2012) Dielectric and Mossbauer studies of ferroelectric and magnetic phase transitions in A-Site and B-Site substituted multiferroic $\text{PbFe}_{0.5}\text{Nb}_{0.5}\text{O}_3$. *IEEE Trans Ultrason Ferroelectr Freq Control* 59:1872–1878
31. Singh SP, Yusuf SM, Yoon S, Baik S, Shin N, Pandey D (2010) Ferroic transitions in the multiferroic $(1-x)\text{Pb}(\text{Fe}_{1/2}\text{Nb}_{1/2})\text{O}_3$ – $x\text{PbTiO}_3$ system and its phase diagram. *Acta Mater* 58:5381–5392
32. Laguta VV, Glinchuk MD, Maryško M et al (2013) Effect of the Ba and Ti-doping on the magnetic properties of multiferroic $\text{Pb}(\text{Fe}_{1/2}\text{Nb}_{1/2})\text{O}_3$. *Phys Rev B* 87:064403-1–064403-8
33. Guzdek P, Sikora M, Gora L, Kapusta Cz (2012) Magnetic and magnetoelectric properties of nickel ferrite–lead iron niobate relaxor composites. *J Eur Ceram Soc* 32:2007–2011
34. Campbell IA (1986) Spin glasses and reentrant alloys. *Hyperfine Interact* 27:15–22
35. Albanese G, Watts BE, Leccabue F, Diaz Castanon S (1998) Mossbauer and magnetic studies of $\text{PbFe}_{1-2-x}\text{Cr}_x\text{O}_{19}$ hexagonal ferrites. *J Magn Magn Mater* 184:337–343